Mfge8 diminishes the severity of tissue fibrosis in mice by binding and targeting collagen for uptake by macrophages

Kamran Atabai,[1,2] Sina Jame,[1,2] Nabil Azhar,[1,2] Alex Kuo,[1,2] Michael Lam,[1,2] William McKleroy,[1,2] Greg DeHart,[1,2] Salman Rahman,[1,2] Dee Dee Xia,[1,2] Andrew C. Melton,[1,2] Paul Wolters,[1,2] Claire L. Emson,[3] Scott M. Turner,[3] Zena Werb,[4] and Dean Sheppard[1,2]

[1]Lung Biology Center, Cardiovascular Research Institute, and [2]Department of Medicine, UCSF, San Francisco, California, USA. [3]KineMed Inc., Emeryville, California, USA. [4]Department of Anatomy, UCSF, San Francisco, California, USA.

Milk fat globule epidermal growth factor 8 (Mfge8) is a soluble glycoprotein known to regulate inflammation and immunity by mediating apoptotic cell clearance. Since fibrosis can occur as a result of exaggerated apoptosis and inflammation, we set out to investigate the hypothesis that Mfge8 might negatively regulate tissue fibrosis. We report here that Mfge8 does decrease the severity of tissue fibrosis in a mouse model of pulmonary fibrosis; however, it does so not through effects on inflammation and apoptotic cell clearance, but by binding and targeting collagen for cellular uptake through its discoidin domains. Initial analysis revealed that *Mfge8*$^{-/-}$ mice exhibited enhanced pulmonary fibrosis after bleomycin-induced lung injury. However, they did not have increased inflammation or impaired apoptotic cell clearance after lung injury compared with *Mfge8*$^{+/+}$ mice; rather, they had a defect in collagen turnover. Further experiments indicated that Mfge8 directly bound collagen and that *Mfge8*$^{-/-}$ macrophages exhibited defective collagen uptake that could be rescued by recombinant Mfge8 containing at least one discoidin domain. These data demonstrate a critical role for Mfge8 in decreasing the severity of murine tissue fibrosis by facilitating the removal of accumulated collagen.

Introduction

Fibrotic diseases are characterized by replacement of normal tissue architecture with collagen-rich matrix, disrupting organ function (1–4). In the lung, fibrosis can occur due to abnormal remodeling after acute lung injury, in the setting of systemic autoimmune and inflammatory disease, or as an idiopathic process (5). The production, deposition, and removal of collagen are dynamic processes, with the balance between collagen production and removal determining tissue architecture (6). When persistent collagen production outpaces or overwhelms mechanisms that remove collagen, excess collagen is deposited in the extracellular matrix, leading to tissue fibrosis.

The molecular pathways responsible for collagen turnover remain incompletely described. Collagen turnover occurs by two pathways, extracellular proteolytic cleavage (7) and endocytosis followed by lysosomal degradation (6). Extracellular collagen cleavage facilitates subsequent intracellular uptake (8). Very little is known about molecules that mediate collagen endocytosis.

Milk fat globule epidermal growth factor 8 (Mfge8) is a soluble glycoprotein that negatively regulates inflammation and autoimmunity by facilitating the clearance of apoptotic cells (9–11). Since fibrosis can occur as a consequence of exaggerated apoptosis and inflammation (12, 13), we hypothesized that Mfge8 may function as a negative regulator of tissue fibrosis. In this report, we show that mice deficient in Mfge8 (*Mfge8*$^{-/-}$ mice) develop exaggerated pulmonary fibrosis after bleomycin treatment. Surprisingly, however, this phenotype is not a consequence of impaired apoptotic cell clearance, exaggerated inflammation, or a more severe acute phase of lung injury. Instead, we find that *Mfge8*$^{-/-}$ mice have a defect in collagen turnover in vivo that is caused by a previously unknown role for Mfge8 in binding and targeting collagen for uptake by macrophages. *Mfge8*$^{-/-}$ macrophages have impaired collagen uptake. We further identify the first discoidin domain of Mfge8 as sufficient for collagen binding and internalization. In this work, we show what we believe to be the first pathway by which a secreted glycoprotein binds collagen and targets it for removal from the extracellular matrix.

Results

Mfge8 is expressed throughout the lung, and expression is increased after injury. To determine the lung expression pattern of Mfge8, we stained sections taken from adult *Mfge8*$^{+/+}$ mice with the anti-Mfge8 antibody 4F6 (9). Mfge8 was present in the alveolar interstitium as well as in the pulmonary vasculature (Figure 1, A and B). Alveolar macrophages obtained by bronchoalveolar lavage (BAL) stained positively for Mfge8 (Figure 1C). To determine whether lung injury induced Mfge8 expression, we challenged mice with the chemotherapeutic agent bleomycin. Bleomycin induces an early acute lung injury response (week 1) characterized by vascular leak and inflammation followed by pulmonary fibrosis (14). While by immunohistochemical analysis, all saline-treated alveolar macrophages expressed some Mfge8 (Figure 1C), the intensity of expression was increased 5 days after bleomycin administration (Figure 1D). We also evaluated whole-lung expression of Mfge8. Mfge8 was induced in the first week after injury. Interestingly, increased expression persisted at 14, 21, and 28 days, suggesting a role for Mfge8 in the fibrotic stage of bleomycin injury (Figure 1E). To determine whether the human ortholog of Mfge8, lactadherin (15, 16), was induced in fibrotic disease in humans, we evaluated expression in samples taken from the lungs of patients with idiopathic pulmonary fibrosis

Conflict of interest: S.M. Turner and C.L. Emson received income and research support as employees of KineMed Inc.

Citation for this article: *J. Clin. Invest.* **119**:3713–3722 (2009). doi:10.1172/JCI40053.

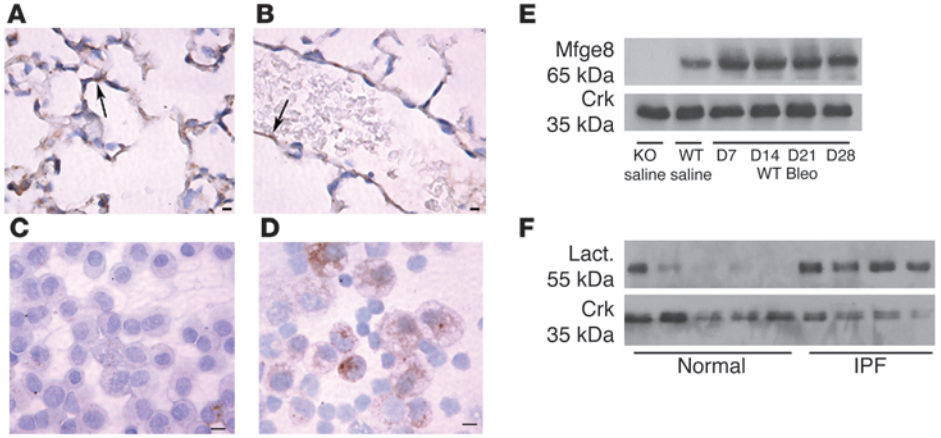

Figure 1
Mfge8 expression is induced by lung injury. (**A** and **B**) Lung sections taken from adult wild-type mice were stained with anti-Mfge8 antibody. Mfge8 was expressed in the alveolar interstitium (arrow in **A**) and pulmonary endothelium (arrow in **B**). Scale bars: 10 μm. (**C** and **D**) Alveolar macrophages were obtained by BAL after saline administration (**C**) or 5 days after bleomycin administration (5 U/kg) (**D**). Mfge8 staining was present in macrophages from saline-treated animals (**C**), and the intensity of expression increased after bleomycin treatment (**D**). Scale bars: 10 μm. (**E**) Ten micrograms of protein from total lung homogenates taken at the indicated days after bleomycin treatment (1.1 U/kg) or 7 days after saline treatment was loaded for a Western blot using an anti-Mfge8 antibody. An antibody against Crk was used to demonstrate equal loading of protein. (**F**) One microgram of protein from lung homogenates obtained from human patients with IPF was loaded for a Western blot using an anti-lactadherin antibody (Lact.). Control samples were from lungs rejected for transplantation. An antibody against Crk was used to demonstrate loading of protein.

(IPF) (Figure 1F). Lactadherin expression was increased in all 4 IPF samples evaluated as compared with control samples taken from nonfibrotic lungs rejected for transplantation.

Mfge8 deficiency results in an exaggerated fibrotic response to bleomycin. Since Mfge8 regulates apoptosis and inflammation, processes closely linked with tissue fibrosis, and bleomycin induces Mfge8 expression in the lung, we evaluated the role of Mfge8 in bleomycin-induced pulmonary fibrosis. *Mfge8*$^{-/-}$ mice were challenged with intratracheal bleomycin (1.1 U/kg), and the severity of pulmonary fibrosis was evaluated at 28 days. Histologically, *Mfge8*$^{-/-}$ mice had more extensive deposition of collagen fibrils than control mice in tissue sections stained with picrosirius red (Figure 2, A and B). To quantify lung fibrosis biochemically, we measured total lung hydroxyproline content 28 days after bleomycin treatment. In our initial phenotypic evaluation, *Mfge8*$^{-/-}$ and control mice were maintained in a mixed-strain background (C57BL/6 × 129/Ola), and we used heterozygous littermates as controls. In these studies, *Mfge8*$^{-/-}$ mice had significantly greater total lung hydroxyproline content than *Mfge8*$^{+/-}$ littermate controls (Figure 2C). Once we had backcrossed mice 6 generations into the C57BL/6 background, we confirmed our phenotype by repeating the measurements of lung hydroxyproline content. *Mfge8*$^{-/-}$ mice had significantly greater fibrosis than *Mfge8*$^{+/+}$ controls 28 days after bleomycin treatment (Figure 2D).

Enhanced fibrosis in Mfge8$^{-/-}$ *mice is not associated with impaired apoptotic cell clearance, increased inflammation, or a more severe acute phase of lung injury*. We next evaluated whether exaggerated fibrosis was associated with impaired apoptotic cell clearance. We first evaluated the efficacy of apoptotic cell clearance in vivo in adult *Mfge8*$^{-/-}$ mice by administering an intratracheal bolus of apoptotic thymocytes. We then quantified the phagocytic index (representing the number of apoptotic cell ingestions per macrophage) of alveolar macrophages obtained by BAL. We found no differences in the phagocytic index between *Mfge8*$^{-/-}$ and control alveolar macrophages (Figure 3A). To evaluate whether Mfge8 was important for in vivo apoptotic cell clearance after lung injury, we stained tissue sections for apoptotic cells with TUNEL. In the early stage (first 24 hours), the majority of apoptotic cells were found in the alveolar epithelium, whereas at subsequent time points the majority were within inflammatory cell infiltrates. At all time points evaluated, we found no significant difference in the number of apoptotic cells in *Mfge8*$^{-/-}$ mice (Figure 3, B and C). After bleomycin treatment but prior to lung harvest, we obtained BAL samples to quantify the in vivo phagocytic index of the alveolar macrophages. Once again, we found no difference in the phagocytic index of *Mfge8*$^{-/-}$ alveolar macrophages (Figure 3, D and E). As another measure of apoptotic cell clearance, we quantified the proportion (Figure 3F) and number (data not shown) of free apoptotic cells recovered by BAL after injury and found no differences. All of these studies except those represented in Figure 3C were carried out in the mixed-strain background using heterozygous control mice. In summary, the exaggerated pulmonary fibrosis in *Mfge8*$^{-/-}$ mice does not appear to be associated with any abnormality in clearance of apoptotic cells from the lung.

We next evaluated the severity of inflammation after bleomycin treatment by quantifying BAL cell number and type. Mfge8 deficiency did not lead to an exaggerated inflammatory response either with high-dose bleomycin (5 U/kg, Supplemental Figure 1A; supplemental material available online with this article; doi:10.1172/JCI40053DS1) used for acute lung injury studies in a mixed-strain background with *Mfge8*$^{+/-}$ controls or bleomycin at a dose used to induce fibrosis (1.1 U/kg, Supplemental Figure 1B) in a pure-strain background using *Mfge8*$^{+/+}$ controls. There were no consistent differences in interstitial inflammation in tissue sections (data not shown) or in the number of infiltrating neutrophils in lung sections as revealed by staining with anti-Gr1 antibody 24 hours after bleomycin administration (Supplemental Figure 1C). We also quantified expression of myeloperoxidase in lung lysates as a marker of neutrophil infiltration 3 days after bleomycin administration and saw no difference between genotypes (Supplemental Figure 1D). As an additional method to evaluate differences in inflammation, we measured gene expression of markers of neutrophils and macrophages 14 days after bleomycin treatment (Supplemental Figure 1E). Though expression of all markers increased in bleomycin- versus saline-treated mice, there were no differences between *Mfge8*$^{-/-}$ and control mice. Next we evaluated the extent of the acute lung injury response by quantifying the severity of lung vascular leak 5 days after bleomycin treatment (5 U/kg) and found no difference

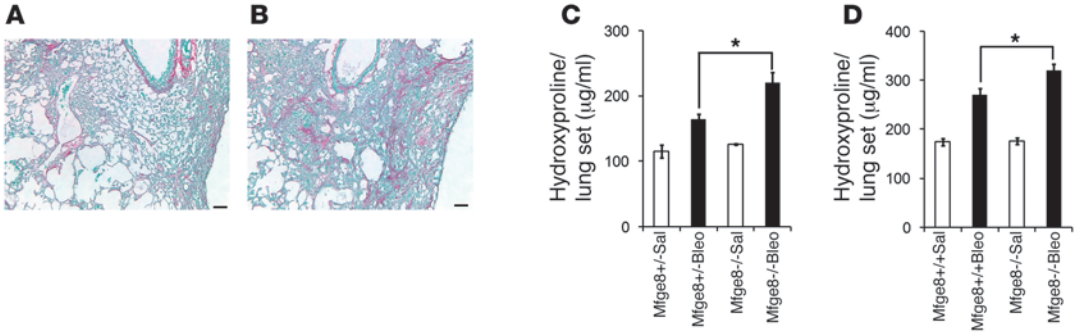

Figure 2

Mfge8$^{-/-}$ mice develop exaggerated pulmonary fibrosis after injury. (**A** and **B**) Picrosirius red staining of lung sections from *Mfge8*$^{+/+}$ (**A**) and *Mfge8*$^{-/-}$ (**B**) mice taken 28 days after bleomycin administration (1.1 U/kg). Scale bars: 100 μm. (**C** and **D**) Biochemical analysis of bleomycin-induced pulmonary fibrosis. Pulmonary fibrosis measured by total lung hydroxyproline content at baseline and 28 days after bleomycin treatment in mice in a mixed-strain background (**C**) or pure-strain background (**D**). Data are presented as mean ± SEM (n = 6–8 for saline [Sal] and 10–14 for bleomycin [Bleo] treatment groups). *P = 0.004 (**C**) and *P = 0.01 (**D**) using Student's t test to compare bleomycin-treated *Mfge8*$^{+/+}$ and *Mfge8*$^{-/-}$ mice.

between *Mfge8*$^{-/-}$ mice (Supplemental Figure 1F) in a mixed-strain background and *Mfge8*$^{+/-}$ controls or *Mfge8*$^{-/-}$ mice (Supplemental Figure 1G) in a pure-strain background and *Mfge8*$^{+/+}$ controls. All subsequent studies were carried out in a pure-strain background with *Mfge8*$^{+/+}$ controls.

Mfge8$^{-/-}$ *mice have impaired collagen degradation in vivo*. An increase in lung hydroxyproline content after injury can represent an increase in production or a defect in turnover of collagen. To determine whether Mfge8 deficiency led to an increase in collagen production, we measured procollagen transcript production by gene expression array 14 days after bleomycin injury (1.1 U/kg) (17, 18). While bleomycin induced the expression of multiple procollagen transcripts in both *Mfge8*$^{-/-}$ and control mice, the relative induction was similar (Supplemental Figure 2A). We confirmed these results for procollagen 1α transcripts on days 7 and 14 with real-time PCR (Supplemental Figure 2B). To confirm that the lack of differences in procollagen gene transcription indicated quantitatively similar collagen production in bleomycin-challenged *Mfge8*$^{-/-}$ and control mice, we measured the rates of collagen synthesis. We measured collagen synthesis by quantifying incorporation of deuterium into hydroxyproline (19). We replaced the drinking water of mice at the time of bleomycin injection with deuterated water (^2H_2O) for 14 days and then measured the incorporation of deuterium (^2H) into the stable C-H bonds of hydroxyproline in newly synthesized collagen by gas chromatography/mass spectroscopy (GC/MS) (19). Administration of bleomycin induced a significant increase in collagen synthesis; however, consistent with our collagen transcript data, there were no significant differences in the rates of synthesis between *Mfge8*$^{-/-}$ and control mice (Supplemental Figure 2C). Total lung hydroxyproline content at this time point was also similar in *Mfge8*$^{-/-}$ and control mice (Supplemental Figure 2D).

We also evaluated whether *Mfge8*$^{-/-}$ mice had an in vivo increase in myofibroblasts, the cell type that produces collagen after bleomycin-induced injury (20). We found no difference in induction of α–smooth muscle actin expression (a marker of myofibroblasts) (Supplemental Figure 2E) or in the number of myofibroblasts in the lung as determined by immunohistochemical quantification (Supplemental Figure 2F). These data indicate that the increase in fibrosis in *Mfge8*$^{-/-}$ mice was due to a defect in collagen removal rather than an increase in collagen production.

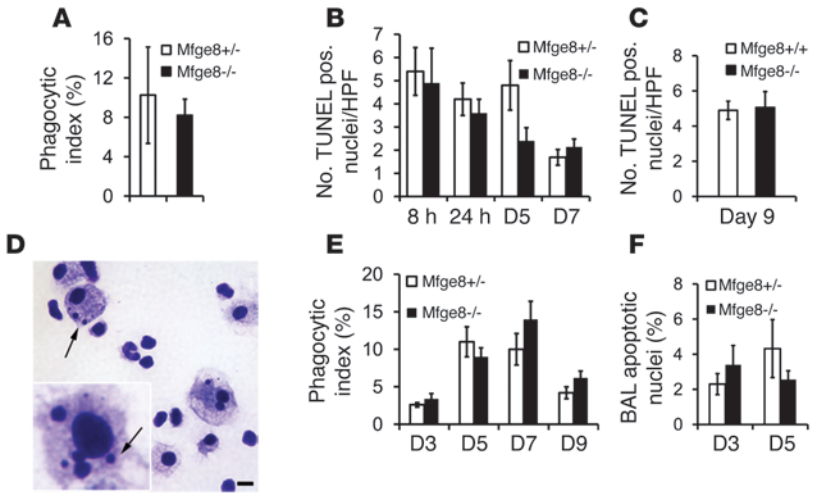

Figure 3

Mfge8$^{-/-}$ mice have intact apoptotic cell clearance in vivo after bleomycin treatment. (**A**) Apoptotic thymocytes were instilled intratracheally and the phagocytic index of alveolar macrophages obtained by BAL 30 minutes after instillation was similar in *Mfge8*$^{-/-}$ and *Mfge8*$^{+/-}$ controls (n = 5–6). (**B**) Tissue sections taken from *Mfge8*$^{-/-}$ and *Mfge8*$^{+/-}$ mice at the indicated hours and days after bleomycin treatment (5 U/kg) were stained by TUNEL assay, and the number of apoptotic cells per ×200 fields (15 fields) was quantified (n = 4–10). (**C**) Sections taken from *Mfge8*$^{-/-}$ and *Mfge8*$^{+/+}$ mice 9 days after bleomycin (1.1 U/kg) treatment were stained by TUNEL as described in **B** (n = 3–4). (**D**–**F**) Cytospin preparations from BAL samples after bleomycin treatment (5 U/kg) were stained with Diff-Quick (**D**) or TUNEL (**F**), and the number of apoptotic cell ingestions (arrows in **D**; and **E**) and percentage of free apoptotic nuclei (**F**) were quantified (n = 5–8). There was no difference in number of TUNEL-positive cells, alveolar macrophage phagocytic index, or free apoptotic nuclei between *Mfge8*$^{-/-}$ and control samples. All comparisons were made using Student's t test, and data are expressed as mean ± SEM.

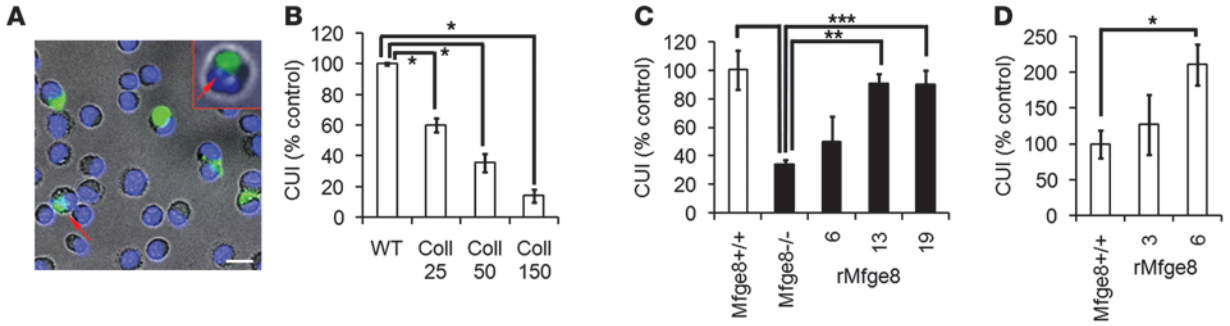

Figure 4

Mfge8 mediates collagen uptake in vitro. (**A**) Primary alveolar macrophages were cultured for 30 minutes with FITC-conjugated type I collagen, and uptake was evaluated by fluorescence microscopy (red arrows). Scale bar: 10 μm. (**B**) Ingestion of collagen was quantified as the collagen uptake index (CUI: number of macrophages with ingestions divided by the total number of macrophages counted). The addition of unlabeled type I collagen (25, 50, 150 μg/ml) inhibited uptake of FITC-conjugated collagen in a dose-dependent fashion (**P* < 0.001, 1-way ANOVA with Bonferroni *t* test for multiple comparisons; *n* = 3–4; data are expressed as percent control relative to wild-type uptake). (**C**) Alveolar macrophages from *Mfge8*$^{-/-}$ mice had significantly impaired collagen uptake index as compared with *Mfge8*$^{+/+}$ alveolar macrophages. (**P* = 0.001, 1-way ANOVA with Bonferroni *t* test for multiple comparisons; *n* = 3–5). Addition of rMfge8 (μg/ml) rescued collagen uptake in *Mfge8*$^{-/-}$ alveolar macrophages (***P* = 0.007, ****P* = 0.023). (**D**) Addition of rMfge8 (μg/ml) increased collagen uptake in *Mfge8*$^{+/+}$ alveolar macrophages under serum-starved conditions (**P* = 0.009, Student's *t* test to compare indicated columns; *n* = 5–6). Data are presented as mean ± SEM.

Mfge8 targets collagen for uptake by macrophages. Collagen is cleaved in the extracellular matrix by proteases and subsequently internalized and degraded in lysosomes (8). Mfge8 contains 2 discoidin domains, homologous to those present in the collagen receptors DDR1 and DDR2 (21). We therefore hypothesized that Mfge8 might bind and mediate uptake of collagen in areas of alveolar scarring. To test this hypothesis, we designed an in vitro collagen phagocytosis assay (Figure 4A). Alveolar macrophages were cultured with FITC-conjugated type I collagen, and internalization of collagen was quantified by fluorescence microscopy. In initial studies (Figure 4B), we showed that addition of increasing doses of type I collagen that was not conjugated with FITC inhibited the uptake of FITC-conjugated collagen in a dose-dependent fashion. We then compared uptake of FITC-conjugated collagen by alveolar macrophages taken from *Mfge8*$^{-/-}$ and *Mfge8*$^{+/+}$ mice. Alveolar macrophages from *Mfge8*$^{-/-}$ mice had significantly impaired collagen uptake as measured by the collagen uptake index (Figure 4C). Addition of recombinant Mfge8 (rMfge8) restored the collagen uptake index to *Mfge8*$^{+/+}$ levels in a dose-dependent fashion (Figure 4C). In the absence of serum, addition of rMfge8 also increased *Mfge8*$^{+/+}$ macrophage collagen uptake index (Figure 4D).

We next evaluated collagen uptake by alveolar macrophages in vivo by placing FITC-conjugated type I collagen into the airways by intratracheal injection. Alveolar macrophages recovered by BAL from *Mfge8*$^{-/-}$ mice had significantly impaired collagen uptake (Figure 5, A and B). In a complementary approach to evaluating in vivo uptake, we quantified the number of retained collagen particles in lung sections after BAL was performed with 10 ml of fluid to remove unbound collagen. There were significantly fewer retained collagen particles in the lung after BAL in *Mfge8*$^{-/-}$ mice (Figure 5, C and D). We next evaluated whether fibroblasts used Mfge8 for collagen uptake in vitro. *Mfge8*$^{-/-}$ lung fibroblasts did not have impaired collagen uptake in vitro, and the addition of rMfge8 did not increase fibroblast collagen uptake (Figure 6, A and B).

Mfge8 deficiency does not affect extracellular collagen degradation. We next evaluated whether proteolytic collagen degradation in the extracellular matrix was affected by Mfge8 deficiency. We measured mRNA transcript levels of proteases with known roles in lung injury and fibrosis 14 days after bleomycin administration by gene expression array (22–24). There were no significant differences in levels of metalloproteinase (MMP); TIMP1; cathepsins B, D, L, and K; or urokinase (Supplemental Figure 3A). We also found no difference in the enzymatic activity of MMP2 and MMP9, two proteases with important roles in lung fibrosis (25–27), by gelatin zymography of lung homogenates taken at 7, 14, 21, and 28 days after bleomycin injury (Supplemental Figure 3B and data not shown). We also evaluated the production of MMP8 (neutrophil collagenase) by Western blot on days 3 and 14 after bleomycin treatment and found no difference between *Mfge8*$^{-/-}$ and control mice (Supplemental Figure 3, C and D).

We were next interested in whether Mfge8 deficiency led to a functional impairment in collagen-degrading capacity in the lung. To answer this question, we evaluated the ability of both alveolar macrophages and bleomycin-treated lung tissue lysates from *Mfge8*$^{-/-}$ and control mice to degrade collagen. The FITC-conjugated collagen molecule is supersaturated with fluorescein such that the close proximity of the fluorescein molecules quenches the fluorescent signal. Proteolytic degradation of collagen results in separation of the fluorescent dye and an increase in the fluorescent signal, which can then be used to quantify collagen cleavage. We therefore cultured alveolar macrophages from *Mfge8*$^{-/-}$ and control mice for 30 minutes with FITC-conjugated type I collagen and measured the fluorescent signal to quantify collagen degradation. We found no difference in collagen degradation between experimental groups (Supplemental Figure 3E). We next evaluated whether lung homogenates had increased collagen-degrading activity by incubating equal concentrations of lung lysates taken from mice 14 and 21 days after bleomycin treatment or saline treatment with FITC-conjugated collagen and measuring degradation by the intensity of the fluorescent signal. In both *Mfge8*$^{-/-}$ and control mice, lung lysates had increased collagen-degrading activity after bleomycin treatment as compared with saline treatment, but there was no significant difference between groups (Supplemental Figure 3F).

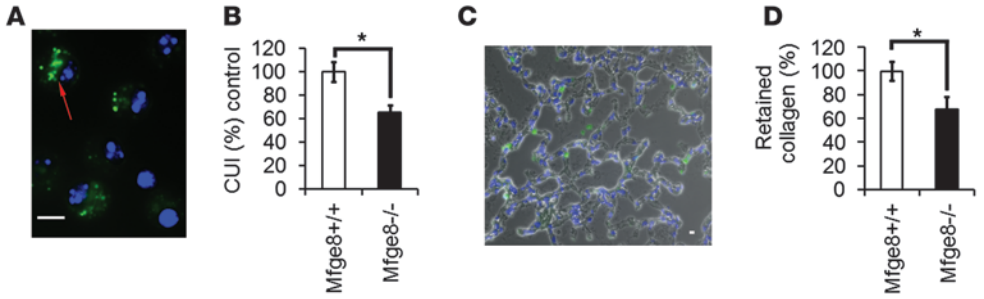

Figure 5
Mfge8 mediates collagen uptake in vivo. (**A**) Alveolar macrophages obtained by BAL 30 minutes after intratracheal injection of FITC-conjugated type I collagen were examined by fluorescence microscopy for collagen uptake (red arrow). Scale bar: 10 μm. (**B**) *Mfge8*$^{-/-}$ alveolar macrophages had significantly impaired collagen uptake in vivo (*P = 0.009, Student's t test; n = 6). (**C**) Frozen sections taken from lungs after intratracheal collagen injection were counterstained with DAPI, and the number of retained collagen particles divided by the total number of nuclei in each section was quantified. Scale bar: 10 μm. (**D**) *Mfge8*$^{-/-}$ lungs retained significantly fewer collagen particles (*P = 0.047 using a Student's t test, n = 4). Data are presented as mean ± SEM.

Mfge8-mediated collagen internalization is independent of RGD-binding integrins. Mfge8 contains an integrin-binding RGD sequence in its second EGF-like domain that is bound by $\alpha_v\beta_3$ or $\alpha_v\beta_5$ integrins (10, 28). These integrins are critical for Mfge8-mediated uptake of apoptotic cells (10, 11). We first confirmed that the $\alpha_v\beta_3$ and $\alpha_v\beta_5$ integrins mediated cell adhesion to rMfge8, whereas other RGD-binding integrins, $\alpha_5\beta_1$, $\alpha_v\beta_6$, or $\alpha_v\beta_8$, did not (data not shown). We then evaluated the roles of $\alpha_v\beta_3$ or $\alpha_v\beta_5$ integrins in Mfge8-mediated collagen uptake. GRGDSP had no effect on collagen uptake in vitro at concentrations up to 10 mM (Supplemental Figure 4A). Alveolar macrophages taken from integrin $\beta5^{-/-}\beta3^{+/-}$ or $\beta5^{-/-}\beta3^{-/-}$ mice had intact collagen uptake in vitro (Supplemental Figure 4B). $\beta5^{-/-}\beta3^{+/-}$ or $\beta5^{-/-}\beta3^{-/-}$ mice did not have an enhanced fibrotic response to bleomycin (Supplemental Figure 4C). These data indicate that Mfge8-mediated collagen endocytosis, in contrast to uptake of apoptotic cells, is independent of RGD binding integrins.

The first discoidin domain of Mfge8 is sufficient for collagen binding and uptake. We next determined the domain of Mfge8 that mediates collagen binding and uptake. Mfge8 contains 2 EGF-like domains at its N terminus and 2 discoidin domains at its C terminus. We created a series of Mfge8 constructs fused to the human Fc (huFc) domain (Figure 7A). We used surface plasmon resonance to evaluate Mfge8-collagen interaction and found a dose-dependent binding of collagen to immobilized full-length Mfge8 construct (Figure 7, B and C). While collagen bound a construct containing only the first discoidin domain of Mfge8 (Dd1) similar to the full-length construct (Figure 7D), collagen did not bind a construct lacking both discoidin domains (Ndd) (Figure 7E). To prove that the first discoidin domain could mediate collagen uptake, we evaluated the ability of each construct to rescue in vitro collagen uptake in *Mfge8*$^{-/-}$ alveolar macrophages. Dd1 significantly increased the collagen uptake index, while the Ndd construct had no significant effect (Figure 7F). These data indicate that the first discoidin domain of Mfge8 is sufficient for collagen binding and uptake.

Discussion

Since its initial description as a milk fat protein, Mfge8 has been shown to have a number of roles, including the regulation of apoptotic cell clearance, autoimmunity, neoangiogenesis, and sperm-egg binding (9, 11, 16, 29). We have found a critical role for Mfge8 in negatively regulating tissue fibrosis mediated by a mechanism that is independent of any of its previously described functions.

Several lines of evidence support a model by which Mfge8 binds collagen that has accumulated in the extracellular space and targets it for uptake and turnover by macrophages. Mfge8 binds collagen directly. *Mfge8*$^{-/-}$ macrophages have impaired collagen internalization in vitro, and this defect is rescued with the addition of rMfge8. *Mfge8*$^{-/-}$ macrophages have impaired collagen uptake in vivo. After bleomycin-induced lung fibrosis, *Mfge8*$^{-/-}$ mice have an increase in total lung collagen content without a relative increase in collagen production.

The content of collagen in the extracellular matrix is precisely regulated by the balance between collagen production and collagen degradation both under homeostatic conditions and in conditions of rapid matrix remodeling such as wound healing. Tissue fibrosis occurs when collagen production outpaces collagen degradation. Several of the molecular processes that result in increased collagen production after injury have been extensively characterized. In lung fibrosis, a paradigm has emerged whereby fibroblasts migrate into damaged air spaces and under the influence of activated TGF-β differentiate into myofibroblasts (30). Myofibroblasts (and fibroblasts) then deposit collagen, producing tissue fibrosis (20). Lysophosphatidic acid (LPA) signaling through the LPA1 receptor recruits fibroblasts into the air spaces (31), while TGF-β promotes both transformation of fibroblasts into myofibroblasts and production of collagen by fibroblasts. The in vivo relevance of these pathways is apparent in that mice deficient in the LPA1 receptor or the $\alpha_v\beta_6$ integrin (a potent activator of TGF-β in the lung) are completely protected from bleomycin-induced lung fibrosis (31, 32).

Surprisingly little is known about the normal homeostatic pathways responsible for collagen removal. In the extracellular matrix, collagen fibers are cleaved and denatured by matrix MMPs (MMP1, MMP13, and MMP14) and further degraded by the gelatinases (MMP2, MMP9) (33–35). The intracellular pathway of collagen degradation involves phagocytosis and lysosomal degradation of collagen by cathepsins (6, 36, 37). MMP cleavage and fragmentation of collagen prior to internalization are also important for this pathway (34), with one group reporting that a much lower rate of internalization can occur despite MMP inhibition (8). A few of the steps involved in collagen uptake by cells have been defined. The $\alpha_2\beta_1$ and $\alpha_3\beta_1$ bind collagen, and inhibition of these integrins reduces phagocytosis of collagen-coated beads (38). The uPARAP/Endo180 receptor, a member of the mannose macrophage receptor family, binds collagen directly, and fibroblasts deficient in this molecule are unable to internalize collagen in vitro (8, 39). Interestingly, in our model Mfge8 does not increase in vitro fibroblast collagen uptake, suggesting that the uPARAP/Endo180 mecha-

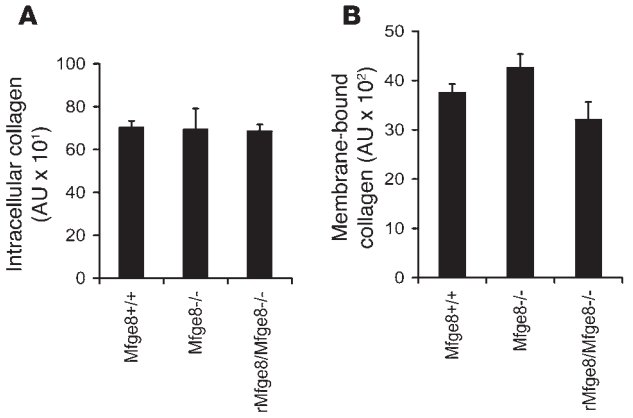

Figure 6

Mfge8$^{-/-}$ fibroblasts do not have impaired collagen uptake. (**A** and **B**) Primary lung fibroblasts from *Mfge8*$^{-/-}$ and *Mfge8*$^{+/+}$ mice at passage 4 were incubated for 90 minutes with FITC-conjugated type I collagen, and unbound/uningested collagen was removed with multiple washes. Cells were then incubated with 50 μg/ml trypsin and 50 μg/ml proteinase K to remove membrane-bound collagen. Collagen in the membrane-bound portion (supernatant after enzymatic treatment) and intracellular portion (pellet remaining after enzymatic treatment) was quantified by a spectrofluorometer. There was no difference in membrane-bound (**A**) or intracellular (**B**) collagen with or without the addition of rMfge8 (13 μg/ml). Data are presented as mean ± SEM.

nism of collagen uptake may be dominant in fibroblasts. The in vivo roles of fibroblast receptors that mediate collagen uptake in regulating tissue fibrosis after injury are unknown.

The results presented here provide the first evidence to our knowledge that an extracellular glycoprotein binds and targets collagen for internalization and intracellular turnover. We have also identified a functional role for the first discoidin domain of Mfge8. The discoidin domains of the cell-surface receptors DDR1 and DDR2 also bind collagen (40, 41). However, binding of collagen by these receptors leads to receptor phosphorylation and downstream signaling rather than collagen ingestion (42). We show what we believe to be the first example of a discoidin domain targeting collagen for cellular uptake.

The second discoidin domain of Mfge8 binds phosphatidylserine residues on apoptotic cells and bridges them to the $\alpha_v\beta_3$ or $\alpha_v\beta_5$ integrins on phagocytes (10, 28). We did not find a role for either of these integrins in collagen phagocytosis. Whether uptake is triggered by a specific receptor or by interaction between Mfge8 and the phagocytic cell surface is unclear. In sperm-egg binding, a model has been proposed by which the first discoidin domain binds sperm and the second domain binds the oocyte, bridging the two together (29). Alternatively, Mfge8 may form dimers through its EGF-like domains, with the discoidin domains serving to bridge sperm to the oocyte (29) or in our case collagen to the macrophage.

It is important to consider whether impaired apoptotic cell clearance in *Mfge8*$^{-/-}$ mice contributed to the increase in fibrosis. Our initial hypothesis was that impaired clearance of apoptotic cells may directly induce fibrosis, and we had set out to investigate the relationship between apoptosis and fibrosis (12). Based on our work in the mammary gland and the work of others (9–11), we expected to see a role for Mfge8 in apoptotic cell clearance after injury in the lung. We could not, however, find evidence of impaired in vivo apoptotic cell clearance in the lungs of bleomycin-treated *Mfge8*$^{-/-}$ mice.

The lack of an absolute increase in apoptotic cell numbers does not exclude the possibility that alternate pathways of clearance could have induced pulmonary fibrosis while still removing apoptotic cells in a timely manner. Several recent publications have shown that Mfge8-independent apoptotic cell clearance induces phagocyte release of IL-1β and IL-6 (43, 44), cytokines that induce inflammation and fibrosis (45, 46). Conversely, Mfge8-dependent apoptotic cell clearance has been shown to induce the release of TGF-β, a profibrotic and antiinflammatory cytokine (32, 44). We found no increase in tissue inflammation after bleomycin administration in *Mfge8*$^{-/-}$ mice, indicating that cytokine-induced inflammation is not likely to be the explanation for increased fibrosis. Furthermore, an increase in fibrosis due to excessive inflammation or TGF-β release and activation would occur through increases in myofibroblast accumulation and collagen production. Our findings indicate that Mfge8 deficiency does not result in increased myofibroblast accumulation or collagen production. Furthermore, Mfge8-independent apoptotic cell clearance would be expected to result in less, not more, TGF-β production, so the effects of loss of Mfge8 on this pathway would be expected to protect against the development of fibrosis.

Another important consideration is whether partially cleaved but uncleared collagen fragments could have induced neutrophilic inflammation by acting as chemoattractants in the lung (47, 48). Our data suggest that this did not occur in bleomycin-treated *Mfge8*$^{-/-}$ mice, since we could not find an increase in lung neutrophils or inflammation-induced increases in collagen production.

The fact that wild-type mice make Mfge8 in response to bleomycin and do develop fibrosis (albeit to a lesser extent than their knockout counterparts) indicates that Mfge8-dependent collagen clearance is a pathway that can be saturated with persistent collagen production. A similar pattern is apparent in lung samples of patients with IPF, all of which have increased expression of the human ortholog of Mfge8, lactadherin (16). Whether pathological fibrosis occurs simply due to overwhelming collagen production or a combination of persistent collagen production coupled with impaired collagen degradation has yet to be determined. Interestingly, in some forms of pharmaceutically induced fibrosis, the phagocytic capacity of fibroblasts is severely reduced, suggesting that collagen turnover pathways can be inhibited (49, 50). As we learn more about the pathways responsible for remodeling and removal of collagen from the extracellular matrix, we can begin to dissect out the relative contribution of increased collagen production and impaired collagen degradation to fibrotic disease. The high prevalence and lack of treatment for fibrotic diseases underscore the importance of a better understanding of the endogenous pathways that mediate removal of collagen from the extracellular matrix.

Methods

Reagents. The rabbit anti-Mfge8 monoclonal antibody (4F6) (9) was used for immunohistochemistry, and anti-Mfge8 antibody from R&D was used for Western blotting. Lactadherin antibody was purchased from R&D; Crk antibody was purchased from BD Biosciences; MMP8 and myeloperoxidase heavy chain antibodies were purchased from Santa Cruz Biotechnology Inc.; anti-Gr1 antibody was purchased from eBioscience; and α–smooth muscle antibody was purchased from Sigma-Aldrich. FITC–

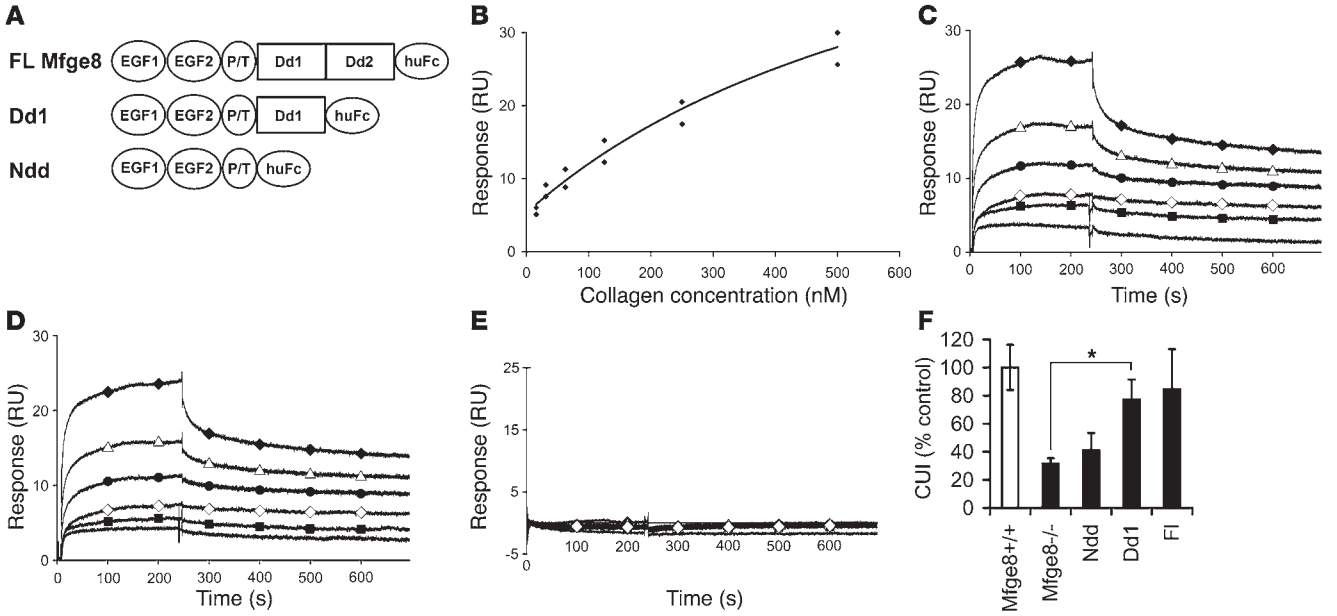

Figure 7

The first discoidin domain of Mfge8 is sufficient for collagen binding and uptake. (**A**) Constructs containing full-length (Fl) Mfge8, Mfge8 lacking the terminal discoidin domain (Dd1), or both discoidin domains (Ndd) fused to a huFc domain were immobilized on a Biacore CM5 chip, and binding to increasing doses of collagen was evaluated. P/T represents a domain present in the long isoform of Mfge8 that is rich in proline and threonine. (**B**) Collagen bound full-length Mfge8 in a dose-dependent fashion with a K_d of 733 nM. (**C**) Flow plot demonstrating dose-dependent binding of collagen to immobilized full-length construct. Black line, 16 nM; filled squares, 31 nM; open diamonds, 63 nM; filled circles, 125 nM; open triangles, 250 nM; filled diamonds, 500 nM. (**D**) Flow plot demonstrating dose-dependent binding of collagen to immobilized Dd1 construct. (**E**) Flow plot demonstrating no binding of collagen to the Ndd construct. (**F**) The ability of constructs (13 μg/ml) to rescue the defect in alveolar macrophage collagen uptake was evaluated in vitro. Dd1 construct rescued *Mfge8*$^{-/-}$ alveolar macrophage collagen uptake, while the Ndd construct had no significant effect (*P = 0.01, 1-way ANOVA with Bonferroni t test; n = 3–4). Data are presented as mean ± SEM.

collagen type I was purchased from Invitrogen and rat tail type I collagen from Sigma-Aldrich. rMfge8 was purchased from R&D. GRGDSP and GRGESP were purchased from Anaspec.

Mfge8-deficient mice. Mice functionally deficient in Mfge8 were created using a gene trap vector and have been previously characterized (9, 16). Initial studies were conducted in a mixed-strain background (C57BL/6 × 129/Ola *Mfge8*$^{+/-}$ littermates used as controls), and subsequent studies were conducted in mice backcrossed 6 or 10 generations into the C57BL/6 background (*Mfge8*$^{+/+}$ used as controls) or 10 generations into the 129/SvEv background. Mice in the 129/SvEv background were used only in studies in Supplemental Figure 4. All experimental protocols were approved by the UCSF IACUC for animal studies.

Tissue sample accrual and processing. Written informed consent was obtained from all subjects, and the study was approved by the UCSF Committee on Human Research. IPF lung tissues were obtained at the time of diagnostic lung biopsy. IPF patients underwent a history, physical examination, high-resolution computed tomography, pulmonary function testing, and diagnostic lung biopsy. In all cases, the pathologic diagnosis was usual interstitial pneumonia (UIP), and the consensus clinical diagnosis was IPF. Normal human lung tissue was obtained from lungs not used by the Northern California Transplant Donor Network. After harvest, lung tissue was directly snap-frozen in liquid nitrogen. Samples were stored at –80°C until use for experiments. For immunoblotting, frozen lung tissue was pulverized in a stainless steel tissue pulverizer (Fisher Scientific), pre-cooled in liquid nitrogen, then immediately lysed in RIPA buffer prior to separation by SDS-PAGE.

Immunohistochemistry. Tissues were fixed with 4% paraformaldehyde or zinc-based formalin (Z-FIX, ANATECH) and embedded in paraffin, and 5-μm sections were treated with 0.2% trypsin for 15 minutes for antigen retrieval. After blocking for 1 hour with 1% BSA/5% goat serum, sections were incubated at room temperature for 1–2 hours with primary antibody, followed by a biotinylated secondary antibody (Vector) for 45 minutes, followed by ABC reagent (Vector) for 30 minutes and liquid diaminobenzidine (Sigma-Aldrich). Sections were counterstained with hematoxylin or methyl green. α–Smooth muscle actin–positive cells taken from 25 randomly selected high-power fields (×200) were quantified. For frozen sections, lungs were inflated with 1.5 ml of OCT medium after BAL was performed, and 5-μm sections were air dried, washed in PBS, and fixed in acetone. After 1 hour of blocking with 5% rat serum, anti-Gr1 antibody was added for 60 minutes and washed off; Alexa Fluor 594 anti-rat (Invitrogen) was added for 30 minutes and washed off; and sections were coverslipped with anti-fade solution containing DAPI (Vector). The number of Gr1-positive cells per 10 randomly selected ×200 fields was quantified by an investigator blinded to the genotype of tissue sections.

Bleomycin model of pulmonary fibrosis. Eight- to- 10-week-old sex-matched mice were anesthetized, and bleomycin (1.1 U/kg Blenoxane) was instilled directly into the trachea after cut-down. Twenty-eight (C57BL/6 or mixed-strain) or 56 (129/SvEv strain) days after treatment, lungs were removed, homogenized, precipitated with trichloroacetic acid, and baked overnight at 110°C in HCl. Samples were reconstituted with 2 ml of water, and hydroxyproline content was measured using a colorimetric chloramine T assay. Some lungs were inflated with 4% PFA to a pressure of 25 cm H_2O, processed, and embedded in paraffin, and then 5-μm sections were stained with picrosirius red for evaluation of fibrosis.

Evaluation of collagen production with deuterated water. Eight- to-10 week-old sex-matched mice were injected with a single bolus i.p. dose of 100% deuterated water (Isotec, Sigma-Aldrich) with 0.9% NaCl, an isosmotic solution delivered at 35 μl/g body mass, at the same time as they received bleomycin. Subsequently, normal drinking water was replaced with 8% deuterated water to maintain the animal's total body water at 5% enrichment of deuterated water for a period of 14 days. Mice were then euthanized, and their lungs removed and processed by mass spectrometry analysis.

Preparation of sample for mass spectrometric analysis. The derivatization of hydroxyproline for GC/MS analysis has been described previously (19). Briefly, tissue was homogenized with a bead mill in normal abundance (non-deuterated) water, and the homogenate was subjected to 2 rounds of acetone precipitation at –20°C in order to obtain the total tissue protein for hydroxyproline assessment. The proteins were hydrolyzed by incubation in 6N HCl, dried under vacuum, and then suspended in a solution of 50% acetonitrile, 50 mM K_2HPO_4, and pentafluorobenzyl bromide before incubation. Derivatives were extracted into ethyl acetate, and the top layer was removed and dried by vacuum centrifugation. In order to acetylate the hydroxyl moiety of hydroxyproline, we incubated samples with a solution of acetonitrile, *N*-methyl-*N*-[*tert*-butyldimethyl-silyl]trifluoroacetamide, and methylimidazole. This material was extracted in petroleum ether and dried with Na_2SO_4.

GC/MS analysis of derivatized hydroxyproline. Analysis of the derivatized hydroxyproline was performed on a standard quadrupole GC/MS instrument (Agilent 5973/6980) in negative chemical ionization mode (NCI-GC/MS), with helium as carrier and methane as reagent gas. The column used was a DB17 ZB-50 column (J&W Scientific, Agilent). Selected ion monitoring was performed on ions with mass-to-charge ratios (m/z) of 424 and 425, which will include all of the carbon-hydrogen bonds from hydroxyproline. The mole fraction of the M1 mass isotopomer was calculated as the ratio of peak areas: M1/(M0 + M1). Incorporation of ^2H into hydroxyproline was calculated as the excess mole fraction of M1 (EM1) above the M1 mole fraction in unlabeled standards at the same abundance. Fractional turnover (*f*), the fraction of newly synthesized hydroxyproline, was calculated as EM1/EM1*, where EM1* represents the EM1 of a newly synthesized molecule. EM1* was calculated from measured body water ^2H_2O enrichments as previously described (19).

Analysis of body ^2H_2O enrichments in body water. ^2H_2O enrichment in plasma samples was measured as previously described (51) using a Series 3000 Cycloidal mass spectrometer (Monitor Instruments).

Evaluation of phagocytic index in vivo. Mice were treated with bleomycin, and at indicated time points alveolar macrophages were obtained by BAL. Cytospin preparations were stained with Diff-Quick (Fisher Scientific) and the number of ingestions per macrophage quantified. The phagocytic index represents the number of ingestions per macrophages counted. A minimum of 300 macrophages were counted, and the investigator was blinded to the genotype of each sample.

BAL. Mice were euthanized, the trachea cannulated, and serial 0.9-ml lavage was performed with ice cold PBS with 1 mM EDTA for a total of 4.5 ml for evaluation of inflammation after bleomycin treatment. Cells were treated with rbc lysis buffer, after which a cell count was obtained by hemocytometer. Cytospin slides were prepared and stained with Diff-Quick reagent and the percentage of inflammatory cell types determined using a light microscope (Supplemental Figure 1, A and B).

TUNEL assay. Five-micrometer sections taken from mice treated with bleomycin were stained with TUNEL assay (ApopTag, Chemicon), and the number of apoptotic cells taken from 15 randomly selected high-power fields (×200) was quantified. For determination of the number of free apoptotic cells recovered by BAL, cytospin preparations were stained with TUNEL assay and the number and proportion of apoptotic cells quantified.

Expression arrays/real-time PCR. Seven and 14 days after treatment with bleomycin (1.1 U/kg), mice were sacrificed, and lungs were removed and RNA extracted using a QIAGEN RNeasy Midi kit following the manufacturer's instructions. After confirming acceptable RNA quality with Agilent nanotechnology, expression arrays were done using an Agilent Mouse One-Color 4×44 K array platform by the UCSF Functional Genomics Core Facility. Complementary DNA was generated from total RNA using a first-strand cDNA synthesis kit (Invitrogen). Real-time PCR was performed using SYBR Green PCR Master Mix (Invitrogen) and results analyzed on an AB Prism 7700 analyzer (Applied Biosystems). Real-time PCR values were normalized to β-actin RNA and expressed as fold increase in mRNA above saline-treated controls.

Collagen uptake assay. Freshly isolated alveolar macrophages were cultured for 60 minutes on glass inserts and RPMI with 0.1% BSA in either 10% mouse serum from the same genotype (Figure 4, B and C, Figure 7F, and Supplemental Figure 4, A and B) or under serum-free conditions (Figure 4D). FITC-conjugated type I collagen (50 μg/ml) was added for 30 minutes at 37°C. After 30 minutes, inserts were washed several times to remove unbound/uningested collagen, counterstained with DAPI, and mounted on slides. Slides were examined with fluorescence microscopy using a Leica DM 5000B camera with Spot 4.5 acquisition software; images were obtained at ×200 magnification, and a minimum of 500 cells were analyzed for evidence of collagen binding/ingestion. Investigators were blinded to the experimental conditions when quantifying collagen uptake. The collagen uptake index represented the number of ingestions per macrophages counted and was expressed as percentage of wild-type uptake. Absolute uptake numbers ranged from 1.5% to 4% for wild-type macrophages. Only cells that visually had collagen surrounded by a rim of cytoplasm were considered to have uptake. The software program Merge 2 (Venning Graphic Utilities) was used to merge images of FITC (representing collagen) and phase contrast (to see cytoplasm) to determine whether collagen was internalized. In preliminary studies, cells that were visually considered as having uptake were further analyzed with Z-plane stacked imaging using a Leica CTR 6000 camera and Image-Pro 5.1 (Media Cybernetics) acquisition software to determine whether collagen was ingested or bound. For collagen to be considered ingested, the maximum fluorescence signal of the FITC (representing collagen) and DAPI (representing macrophage nuclei) had to be present at the same level, and there had to be a clear rim of cytoplasm between the FITC signal and the outside of the cell. Using these criteria, 70% of cells (of 100 counted) that were considered to have uptake by visual analysis had uptake according to Z-plane analysis. Therefore, the in vitro collagen uptake index represents both ingested (70%) and bound (30%) collagen.

For all inhibitor studies and studies with recombinant protein, compounds were added to macrophages 30 minutes prior to initiation of the uptake assay.

For the in vivo uptake assay, 60 μg of collagen in 60 μl H_2O was placed intratracheally; 30 minutes later, alveolar macrophages were recovered by BAL and cytospin preparations made with DAPI counterstain, and the proportion of macrophages with ingestions was quantified by fluorescence microscopy and expressed as percent control of wild-type macrophage uptake. The actual percentage of wild-type macrophage uptake in vivo was 39. Mouse lungs were further lavaged with 10 ml PBS to remove residual collagen and then inflated with 1.5 cc of OCT medium and prepared for frozen sectioning. Five-micrometer sections were counterstained with DAPI, and the number of collagen particles per total number of nuclei counted in the section was quantified from 5 randomly selected high-power fields (×200) and expressed as percent control of wild-type. The actual proportion of retained nuclei in wild-type sections was 15%.

Fibroblast collagen uptake assay. For fibroblast uptake assays, lung fibroblasts were isolated by digesting whole lung with Blendzyme 3 (Roche). After 4 passages in vitro, fibroblasts were plated at a concentration of 50,000 cells per 24-well plate overnight in 10% FCS DMEM. Fibroblasts were then washed 3 times with PBS and incubated in media containing 10% mouse serum of the same genotype as the fibroblasts. FITC-conjugated type I collagen (50 μg/ml) was added for 90 minutes, after which the cells were washed vigorously with PBS. Fibroblasts were then incubated with 50 μg/ml trypsin and 50 μg/ml proteinase K at 37°C for 5 minutes, after which they were removed and centrifuged, and the supernatant containing the membrane-bound collagen cleaved by proteolytic treatment was separated. The remaining pellet was lysed with 0.1 M NaOH to release intracellular collagen, and fluorescence was measured in both the supernatant and pellet using a spectrofluorometer (Tecan).

Collagen degradation assays. For the in vitro assay, isolated alveolar macrophages were cultured in black 96-well black plates in triplicate. Cells were plated at a concentration of 50,000 cells per well in PBS with 1 μg/ml of FITC-conjugated type I collagen (Invitrogen) in a total volume of 100 μl. The FITC-conjugated collagen from Invitrogen is designed for enzymatic assays and is supersaturated with FITC. When the collagen is cleaved, the fluorescent signal increases. After 30 minutes, fluorescence was quantified using a spectrofluorometer (Tecan). The fluorescent signal from control wells containing only collagen was subtracted from that from wells containing macrophages and collagen.

For the assay using in vivo samples, 10 μg of total lung homogenates from saline- and bleomycin-treated mice were incubated at 37°C with FITC-conjugated type I collagen (10 μg/ml) in duplicate. After 60 minutes, fluorescence was quantified using a spectrofluorometer (Tecan). The fluorescent signal from control wells containing only collagen was subtracted from that from wells containing tissue lysates and collagen.

Mfge8 constructs. RNA taken from the involuting mouse mammary gland was extracted using TRIzol following the manufacturer's instructions (Invitrogen). Full-length Mfge8 was cloned into the pMIB/V5-His vector (Invitrogen) using the sequences 5′-GGCATGCTAAGCTTGTCTGGTGACTTCTGTGACTCCAGCCTGTGC-3′ (Mfge8 forward primer) and 5′-GGCGGCACTAGTTCTGCCTTCGATACAGCCCAGCAGCTCCAG-3′ (Mfge8 reverse primer). The huFc domain was cloned into the vector using the sequences 5′-GGCGGCACTAGTGCACCTGAACTCCTGGGGGGACCGTC-3′ (Fc forward primer) and 5′-TATCTGCAGAATTCTCATTTACCCGGAGACAGGGAGAGGCTC-3′ (Fc reverse primer). For the Dd1 and Ndd construct, the primers 5′-GGCATGCTAAGCTTGTCTGGTGACTTCTGTGACTCCAGCCTGTGC-3′ (Mfge8 forward primer), 5′-GGCGGCACTAGTTCTGCCTTCGATGCCCAGGAGCTCGAAGCG-3′ (Dd1 reverse primer), and 5′-GGCGGCACTAGTTCTGCCTTCGATGGAGGCTAGGTTGTTGGA-3′ (Ndd reverse primer) were used to obtain cDNA that was then inserted into the pMIB/V5-His vector containing huFc after enzymatic digestion and removal of the full-length construct. High Five cells were transfected with each vector using Cellfectin reagent (Invitrogen) and recombinant protein isolated by binding on a protein G column and eluting with a pH gradient.

Surface plasmon resonance. Proteins were immobilized on different flow cells of a Biacore CM5 chip and analyzed on a Biacore T100. The dextran surface on the chip was first activated by injection of a 1:1 mixture of *N*-hydroxysuccinimide and *N*-ethyl-*NP*-[(3-dimethylamino)-propyl]-carbodiimide hydrochloride (GE Healthcare). Proteins were then diluted to 20 μg/ml in 10 mM sodium acetate at pH 4.5 and injected to equal mass density of 3,000 response units (RU) on the surface. The remaining active sites on the surface were then blocked with 1 M ethanolamine-HCl, and washed with HEPES-buffered saline with 0.05% P-20. Type I collagen was diluted into running buffer (PBS with 0.05% Tween-20) and injected at different concentrations at a flow rate of 30 μl/min in duplicate with intermittent blank injections of running buffer alone. The surfaces were regenerated after each injection to remove residual bound collagen by injection of 2 M NaCl and washing with running buffer. The response for each flow cell was represented in reference to a flow cell with EGFR1-Fc immobilized and subtracted by the average response of the blank injections over each surface.

Evaluation of vascular permeability. Five days after treatment with intratracheal bleomycin (5 U/kg), mice were administered 0.5 μCi of [^{125}I]albumin by i.p. injection. Four hours later, they were sacrificed and their lungs removed and homogenized. A blood sample was used to calculate the hematocrit. Vascular permeability was expressed as extravascular plasma equivalents (EVPE), the ratio of radioactive counts in the lung (after subtraction of counts attributable to the blood content within the lung) to counts in the plasma (52).

Statistics. Paired data columns were evaluated using Student's *t* test with Microsoft Office Excel 2007. One-way ANOVA was used for comparison of multiple data columns using SigmaStat 3.11 (SYSTAT), and when differences were statistically significant, this was followed with a Bonferroni *t* test for subsequent pairwise analysis. Data were tested for normality and variance, and a *P* value less than 0.05 was considered significant.

Acknowledgments

This work was supported by NIH grants HL64353 HL53949, HL083950, AI024674, and NIH Program in Genomics Applications grant (BayGenomics) HL66600 (to D. Sheppard), NIH grant AI053194 (to Z. Werb), NIH K08 mentored award HL083985 (to K. Atabai), and an American Lung Association Biomedical Research Grant (to K. Atabai). We thank Robert Fletterick (NIH grant S10 RR023443) and the Sandler Foundation for providing access to and assistance with measurement of surface plasmon resonance and Mark Looney and Michael Matthay for help with vascular permeability studies.

Received for publication June 1, 2009, and accepted in revised form September 9, 2009.

Address correspondence to: Dean Sheppard, Lung Biology Center, box 2922, UCSF, San Francisco, California 94143, USA. Phone: (415) 514-4269; Fax: (415) 514-4278; E-mail: Dean.Sheppard@UCSF.edu.

1. Raghu, G., Striker, L.J., Hudson, L.D., and Striker, G.E. 1985. Extracellular matrix in normal and fibrotic human lungs. *Am. Rev. Respir. Dis.* **131**:281–289.
2. Chua, F., Gauldie, J., and Laurent, G.J. 2005. Pulmonary fibrosis: searching for model answers. *Am. J. Respir. Cell Mol. Biol.* **33**:9–13.
3. Hammar, S.P., Winterbauer, R.H., Bockus, D., Remington, F., and Friedman, S. 1985. Idiopathic fibrosing alveolitis: a review with emphasis on ultrastructural and immunohistochemical features. *Ultrastruct. Pathol.* **9**:345–372.
4. Wynn, T.A. 2008. Cellular and molecular mechanisms of fibrosis. *J. Pathol.* **214**:199–210.
5. Gross, T.J., and Hunninghake, G.W. 2001. Idiopathic pulmonary fibrosis. *N. Engl. J. Med.* **345**:517–525.
6. Everts, V., van der Zee, E., Creemers, L., and Beertsen, W. 1996. Phagocytosis and intracellular digestion of collagen, its role in turnover and remodelling. *Histochem. J.* **28**:229–245.
7. Song, F., Wisithphrom, K., Zhou, J., and Windsor, L.J. 2006. Matrix metalloproteinase dependent and independent collagen degradation. *Front. Biosci.* **11**:3100–3120.
8. Madsen, D.H., et al. 2007. Extracellular collagenases and the endocytic receptor, urokinase plasminogen activator receptor-associated protein/Endo180, cooperate in fibroblast-mediated collagen degradation. *J. Biol. Chem.* **282**:27037–27045.
9. Atabai, K., et al. 2005. Mfge8 is critical for mammary gland remodeling during involution. *Mol. Biol. Cell.* **16**:5528–5537.
10. Hanayama, R., et al. 2002. Identification of a factor that links apoptotic cells to phagocytes. *Nature.* **417**:182–187.

11. Hanayama, R., et al. 2004. Autoimmune disease and impaired uptake of apoptotic cells in MFG-E8-deficient mice. *Science.* **304**:1147–1150.
12. Teder, P., et al. 2002. Resolution of lung inflammation by CD44. *Science.* **296**:155–158.
13. Kuwano, K., et al. 1999. Essential roles of the Fas-Fas ligand pathway in the development of pulmonary fibrosis. *J. Clin. Invest.* **104**:13–19.
14. Hay, J., Shahzeidi, S., and Laurent, G. 1991. Mechanisms of bleomycin-induced lung damage. *Arch. Toxicol.* **65**:81–94.
15. Veron, P., Segura, E., Sugano, G., Amigorena, S., and Thery, C. 2005. Accumulation of MFG-E8/lactadherin on exosomes from immature dendritic cells. *Blood Cells Mol. Dis.* **35**:81–88.
16. Silvestre, J.S., et al. 2005. Lactadherin promotes VEGF-dependent neovascularization. *Nat. Med.* **11**:499–506.
17. Kaminski, N., et al. 2000. Global analysis of gene expression in pulmonary fibrosis reveals distinct programs regulating lung inflammation and fibrosis. *Proc. Natl. Acad. Sci. U. S. A.* **97**:1778–1783.
18. Shahzeidi, S., Jeffery, P.K., Laurent, G.J., and McAnulty, R.J. 1994. Increased type I procollagen mRNA transcripts in the lungs of mice during the development of bleomycin-induced fibrosis. *Eur. Respir. J.* **7**:1938–1943.
19. Gardner, J.L., et al. 2007. Measurement of liver collagen synthesis by heavy water labeling: effects of profibrotic toxicants and antifibrotic interventions. *Am. J. Physiol. Gastrointest. Liver Physiol.* **292**:G1695–G1705.
20. Zhang, K., Rekhter, M.D., Gordon, D., and Phan, S.H. 1994. Myofibroblasts and their role in lung collagen gene expression during pulmonary fibrosis. A combined immunohistochemical and in situ hybridization study. *Am. J. Pathol.* **145**:114–125.
21. Vogel, W., Gish, G.D., Alves, F., and Pawson, T. 1997. The discoidin domain receptor tyrosine kinases are activated by collagen. *Mol. Cell.* **1**:13–23.
22. Kimura, M., et al. 2005. The significance of cathepsins, thrombin and aminopeptidase in diffuse interstitial lung diseases. *J. Med. Invest.* **52**:93–100.
23. Sisson, T.H., and Simon, R.H. 2007. The plasminogen activation system in lung disease. *Curr. Drug Targets.* **8**:1016–1029.
24. Winkler, M.K., and Fowlkes, J.L. 2002. Metalloproteinase and growth factor interactions: do they play a role in pulmonary fibrosis? *Am. J. Physiol. Lung Cell Mol. Physiol.* **283**:L1–L11.
25. Garcia-Alvarez, J., et al. 2006. Membrane type-matrix metalloproteinases in idiopathic pulmonary fibrosis. *Sarcoidosis Vasc. Diffuse Lung Dis.* **23**:13–21.
26. Cabrera, S., et al. 2007. Overexpression of MMP9 in macrophages attenuates pulmonary fibrosis induced by bleomycin. *Int. J. Biochem. Cell Biol.* **39**:2324–2338.
27. Betsuyaku, T., Fukuda, Y., Parks, W.C., Shipley, J.M., and Senior, R.M. 2000. Gelatinase B is required for alveolar bronchiolization after intratracheal bleomycin. *Am. J. Pathol.* **157**:525–535.
28. Nandrot, E.F., et al. 2007. Essential role for MFG-E8 as ligand for alphavbeta5 integrin in diurnal retinal phagocytosis. *Proc. Natl. Acad. Sci. U. S. A.* **104**:12005–12010.
29. Ensslin, M.A., and Shur, B.D. 2003. Identification of mouse sperm SED1, a bimotif EGF repeat and discoidin-domain protein involved in sperm-egg binding. *Cell.* **114**:405–417.
30. Fine, A., and Goldstein, R.H. 1987. The effect of transforming growth factor-beta on cell proliferation and collagen formation by lung fibroblasts. *J. Biol. Chem.* **262**:3897–3902.
31. Tager, A.M., et al. 2008. The lysophosphatidic acid receptor LPA1 links pulmonary fibrosis to lung injury by mediating fibroblast recruitment and vascular leak. *Nat. Med.* **14**:45–54.
32. Munger, J.S., et al. 1999. The integrin alpha v beta 6 binds and activates latent TGF beta 1: a mechanism for regulating pulmonary inflammation and fibrosis. *Cell.* **96**:319–328.
33. Egeblad, M., and Werb, Z. 2002. New functions for the matrix metalloproteinases in cancer progression. *Nat. Rev. Cancer.* **2**:161–174.
34. Lee, H., Overall, C.M., McCulloch, C.A., and Sodek, J. 2006. A critical role for the membrane-type 1 matrix metalloproteinase in collagen phagocytosis. *Mol. Biol. Cell.* **17**:4812–4826.
35. Visse, R., and Nagase, H. 2003. Matrix metalloproteinases and tissue inhibitors of metalloproteinases: structure, function, and biochemistry. *Circ. Res.* **92**:827–839.
36. Dyer, R.F., and Peppler, R.D. 1977. Intracellular collagen in the nonpregnant and IUD-containing rat uterus. *Anat. Rec.* **187**:241–247.
37. Melcher, A.H., and Chan, J. 1981. Phagocytosis and digestion of collagen by gingival fibroblasts in vivo: a study of serial sections. *J. Ultrastruct. Res.* **77**:1–36.
38. Lee, W., Sodek, J., and McCulloch, C.A. 1996. Role of integrins in regulation of collagen phagocytosis by human fibroblasts. *J. Cell. Physiol.* **168**:695–704.
39. Behrendt, N. 2004. The urokinase receptor (uPAR) and the uPAR-associated protein (uPARAP/Endo180): membrane proteins engaged in matrix turnover during tissue remodeling. *Biol. Chem.* **385**:103–136.
40. Leitinger, B. 2003. Molecular analysis of collagen binding by the human discoidin domain receptors, DDR1 and DDR2. Identification of collagen binding sites in DDR2. *J. Biol. Chem.* **278**:16761–16769.
41. Curat, C.A., Eck, M., Dervillez, X., and Vogel, W.F. 2001. Mapping of epitopes in discoidin domain receptor 1 critical for collagen binding. *J. Biol. Chem.* **276**:45952–45958.
42. Vogel, W., et al. 2000. Discoidin domain receptor 1 is activated independently of beta(1) integrin. *J. Biol. Chem.* **275**:5779–5784.
43. Jinushi, M., et al. 2008. Milk fat globule EGF-8 promotes melanoma progression through coordinated Akt and twist signaling in the tumor microenvironment. *Cancer Res.* **68**:8889–8898.
44. Jinushi, M., et al. 2007. MFG-E8-mediated uptake of apoptotic cells by APCs links the pro- and anti-inflammatory activities of GM-CSF. *J. Clin. Invest.* **117**:1902–1913.
45. Gasse, P., et al. 2007. IL-1R1/MyD88 signaling and the inflammasome are essential in pulmonary inflammation and fibrosis in mice. *J. Clin. Invest.* **117**:3786–3799.
46. Saito, F., et al. 2008. Role of interleukin-6 in bleomycin-induced lung inflammatory changes in mice. *Am. J. Respir. Cell Mol. Biol.* **38**:566–571.
47. Riley, D.J., et al. 1988. Neutrophil response following intratracheal instillation of collagen peptides into rat lungs. *Exp. Lung Res.* **14**:549–563.
48. Weathington, N.M., et al. 2006. A novel peptide CXCR ligand derived from extracellular matrix degradation during airway inflammation. *Nat. Med.* **12**:317–323.
49. Kataoka, M., Kido, J., Shinohara, Y., and Nagata, T. 2005. Drug-induced gingival overgrowth — a review. *Biol. Pharm. Bull.* **28**:1817–1821.
50. McGaw, W.T., and Porter, H. 1988. Cyclosporine-induced gingival overgrowth: an ultrastructural stereologic study. *Oral Surg. Oral Med. Oral Pathol.* **65**:186–190.
51. Busch, R., et al. 2006. Measurement of protein turnover rates by heavy water labeling of non-essential amino acids. *Biochim. Biophys. Acta.* **1760**:730–744.
52. Su, X., et al. 2007. Activation of the alpha7 nAChR reduces acid-induced acute lung injury in mice and rats. *Am. J. Respir. Cell Mol. Biol.* **37**:186–192.